Journal of Quantitative Spectroscopy & Radiative Transfer 227 (2019) 47–56

Contents lists available at ScienceDirect

Journal of Quantitative Spectroscopy & Radiative Transfer

journal homepage: www.elsevier.com/locate/jqsrt

Energy levels, transition dipole moment, transition probabilities and radiative lifetimes for low-lying electronic states of PN

Z. Qin[a], J.M. Zhao[a], L.H. Liu[a,b,*]

[a] School of Energy Science and Engineering, Harbin Institute of Technology, Harbin 150001, China
[b] School of Energy and Power Engineering, Shandong University, Qingdao 266237, China

ARTICLE INFO

Article history:
Received 3 January 2019
Revised 2 February 2019
Accepted 2 February 2019
Available online 4 February 2019

Keywords:
Spectroscopic parameters
Transition probabilities
Phosphorus mononitride

ABSTRACT

The valence internally contracted multireference configuration-interaction (icMRCI) method is used to compute potential energy curves (PECs) of the $X^1\Sigma^+$, $A^1\Pi$, $C^1\Sigma^-$, $D^1\Delta$, $2^1\Pi$, $a^3\Sigma^+$, $b^3\Pi$, $d^3\Delta$, $e^3\Sigma^-$, $2^3\Delta$, $2^3\Sigma^-$, $1^5\Sigma^+$ and $1^5\Pi$ states for PN, together with the Davidson, core-valence (CV) and scalar relativistic corrections, as well as the basis-set extrapolation. Transition dipole moments (TDMs) of fifteen dipole-allowed transitions between the thirteen states are calculated by the icMRCI approach with the aug-cc-pV6Z basis set. The vibrational band origins, Einstein coefficients and Franck-Condon factors of all spontaneous emissions for the fifteen band systems are determined, seeking to theoretically predict the strong emissions at least of the order of 10^3 s^{-1} for Einstein coefficients. Comparing with experimental measurements, our calculations can well reproduce the band origins and Franck-Condon factors of the $A^1\Pi$-$X^1\Sigma^+$ system. Similar accuracy is assumed for the other band systems. Many emissions for the $A^1\Pi$-$X^1\Sigma^+$, $2^1\Pi$-$A^1\Pi$, $2^1\Pi$-$X^1\Sigma^+$, $2^1\Pi$-$C^1\Sigma^-$, $2^1\Pi$-$D^1\Delta$, $b^3\Pi$-$a^3\Sigma^+$, $e^3\Sigma^-$-$b^3\Pi$, $2^3\Delta$-$1^3\Delta$, $2^3\Sigma^-$-$1^3\Sigma^-$, $2^3\Sigma^-$-$b^3\Pi$ and $1^5\Pi$-$1^5\Sigma^+$ systems are found to be strong according to our calculated Einstein coefficients, whereas the emissions are weak for the $2^3\Delta$-$b^3\Pi$ system. Radiative lifetimes for the first 15 vibrational levels are evaluated to be about tens of nanoseconds for the $2^1\Pi$ state, about several hundred nanoseconds for the $A^1\Pi$ state, about several to tens of microseconds for the $b^3\Pi$, $2^3\Delta$, $2^3\Sigma^-$ and $1^5\Pi$ states and about several to several hundred microseconds for the $e^3\Sigma^-$ state. The results can be used as guidelines for line identification and diagnostics of astrophysical plasma.

1. Introduction

Phosphorus mononitride (PN) is the first P-bearing molecule detected in the interstellar medium [1,2]. Subsequently, it was observed in the Origin "plateau" source [3], star-forming regions and cold cloud cores [4]. Over the past ten years or so, PN and other P-bearing species have been discovered by many research groups. These discoveries of P-bearing species, in the oxygen-rich supergiant star VY Canis Majoris [5,6], in the wind of the oxygen-rich AGB star IK Tauri [7], in massive dense cores [8–10], in solar-type star-forming regions [11] and in five molecular clouds located in the Galactic Center [12], greatly enhance our understanding of the interstellar medium, since many emission lines have been observed. It is well known that spectral lines can provide valuable information on astrophysical plasma. Analyzing the observed spectra requires knowledge of the transition properties of PN. However, transition properties between triplet or quintet states of PN have not been investigated experimentally and theoretically.

Experimentally, spectroscopic observation of PN molecule was first reported by Curry et al. [13] for the bands in the region 2400–2900 Å. Analysis of the measured 24 bands gave an assignment of this system as a $^1\Pi$-$^1\Sigma$ transition [14,15]. However, no attention had been paid to PN molecule until 1971 when Raymonda and Klemperer [16] provided a set of complementary structure parameters of PN by analyzing the molecular beam electric resonance spectrum. Since then, a number of experimental studies [17–29] have been performed and lots of spectral bands have been recorded. Most of them are designed to investigate the molecular structure and spectroscopic parameters of PN. In particular, Moeller and Silvers [17] obtained a table of relative transition probabilities of the $A^1\Pi$-$X^1\Sigma^+$ system from the observed fluorescence spectra of PN. Ghosh et al. [20] reported a high resolution study of the $A^1\Pi$-$X^1\Sigma^+$ system in the spectral range of 2200–3100 Å, including $\upsilon' = 0$–10 to $\upsilon'' = 0$–11 transitions. Ahmad and Hamilton [24] reported accurate infrared and microwave results of the $A^1\Pi$-$X^1\Sigma^+$ system. Coquart and Prudhomme [18,19] first observed the absorption spectra of the $E^1\Sigma^+$-$X^1\Sigma^+$ transition in the 1600–

* Corresponding author at: School of Energy and Power Engineering, Shandong University, 72 Binhai Road, Optical and Thermal Radiation Research, Qingdao Shandong, 266237, China.
E-mail address: liulinhua@sdu.edu.cn (L.H. Liu).

https://doi.org/10.1016/j.jqsrt.2019.02.002
0022-4073/

1900 Å region and found 11 vibrational levels of the new excited $E^1\Sigma^+$ state. Verma et al. [22] identified some absorption bands in the spectral region 1300–1500 Å as the $\alpha^1\Pi$-$X^1\Sigma^+$, $\beta^1\Pi$-$X^1\Sigma^+$, $\gamma^1\Sigma^+$-$X^1\Sigma^+$ and $\delta^1\Sigma^+$-$X^1\Sigma^+$ transitions by rotational analysis of these bands. Saraswathy and Krishnamurty [21] carried out a rotational analysis of 11 bands of the $A^1\Pi$-$X^1\Sigma^+$ system for $P^{14}N$ and 16 bands of the $A^1\Pi$-$X^1\Sigma^+$ system for $P^{15}N$, along with the perturbation in the $\upsilon = 0$–4 levels of $A^1\Pi$ state caused by the $e^3\Sigma^-$, $d^3\Delta$ and $b^3\Pi$ states. Such study was improved later by Floch et al. [26]. In addition, Bredohl et al. [23] observed the absorption spectrum of PN up to 1050 Å and determined 5 Rydberg series.

Theoretically, a great deal of work [30–44] has been done on the electronic structure, potential energy and spectroscopic parameters of PN. Among these theoretical studies, only one group investigated the transition properties of PN, i.e., de Brouckere et al. [35,37] determined the pure rotational, rovibrational transitions and spontaneous radiative lifetimes for the $X^1\Sigma^+$ ground state of PN and calculated the Einstein coefficients and Franck-Condon factors of the $A^1\Pi$-$X^1\Sigma^+$ and $D^1\Delta$-$A^1\Pi$ systems.

Analyzing previous experimental results, we can find that many spectral bands have been recorded for the $A^1\Pi$-$X^1\Sigma^+$ system of PN, together with numerous vibrational band origins. Four triplet $a^3\Sigma^+$, $e^3\Sigma^-$, $d^3\Delta$ and $b^3\Pi$ states have been observed by analysis of their perturbation in the $A^1\Pi$ state, but little spectroscopic data of them have been obtained. Experimental observation seems not to have reported the transition properties between triplet or quintet states over the past few decades. We wonder whether the transitions between triplet or quintet states are too weak to observe. Moreover, theoretical studies have not been carried out for radiative transition probabilities between triplet or quintet states. Radiative lifetimes of any triplet or quintet states are not available in the literature. So the transition properties of PN are worthy of further investigation.

This work is organized as follows. In Section 2, we briefly present the theory and method, including the dissociation relationships between the electronic states and the dissociation limits of PN, the approaches of calculating the potential energy curves (PECs) and the transition dipole moments (TDMs), and the formulas of computing the transition parameters. In Section 3, PECs and TDMs are reported. The vibrational band origins, Einstein coefficients of spontaneous emission (hereafter called Einstein coefficients) and Franck-Condon factors are determined for dipole-allowed transition systems. Radiative lifetimes are also evaluated for the $A^1\Pi$, $D^1\Delta$, $2^1\Pi$, $b^3\Pi$, $e^3\Sigma^-$, $2^3\Delta$, $2^3\Sigma^-$ and $1^5\Pi$ states. In Section 4, conclusions are drawn. These results can be used as guidelines for line identification and diagnostics of astrophysical plasma.

2. Theory and method

2.1. Dissociation relationships

The ground states of nitrogen (N) and Phosphorus (P) are $(2p^3)^4S_u$ and $(3p^3)^4S_u$, respectively. The first and second excited states of N are $(2p^3)^2D_u$ and $(2p^3)^2P_u$, respectively. Their energy levels relative to the ground state are 19,228.82 cm^{-1} and 28,839.11 cm^{-1} [45], which are obtained, respectively, by averaging the energy of the $(2p^3)^2D_{3/2}$ and $(2p^3)^2D_{5/2}$ states and by averaging the energy of the $(2p^3)^2P_{1/2}$ and $(2p^3)^2P_{3/2}$ states. The first and second excited states of P are $(3p^3)^2D_u$ and $(3p^3)^2P_u$, respectively. Their energy levels relative to the ground state are 11,368.83 cm^{-1} and 18,735.36 cm^{-1} [45], which are obtained, respectively, by averaging the energy of the $(3p^3)^2D_{1/2}$ and $(3p^3)^2D_{3/2}$ states and by averaging the energy of the $(3p^3)^2P_{1/2}$ and $(3p^3)^2P_{3/2}$ states. Therefore, the first six dissociation limits of PN are $P(^4S_u)$+$N(^4S_u)$, $P(^4D_u)$+$N(^4S_u)$, $P(^2P_u)$+$N(^4S_u)$, $P(^4S_u)$+$N(^2D_u)$, $P(^4S_u)$+$N(^2P_u)$ and $P(^2D_u)$+$N(^2D_u)$, respectively. These six dissociation limits and their generating 54 electronic states are presented in Table 1. The energy separations between each higher dissociation limit and the lowest one are calculated and given in Table 1, which are in excellent agreement with the experimental data [45].

2.2. PECs and TDMs

Using the complete active space self-consistent field (CASSCF) wave functions [46] as reference, PECs are calculated by the internally contracted multireference configuration-interaction (icMRCI) method [47,48] with Davidson correction (+Q). These calculations are done in C_{2v} symmetry and performed in the MOLPRO 2015 program suite [49,50]. In the calculations, nine outermost molecular orbitals (MOs) ($5a_1$, $2b_1$ and $2b_2$), i.e., 5-9σ, 2π and 3π MOs, are chosen as active orbitals. 10 valence electrons of PN are distributed into 9 valence MOs, the other 12 inner electrons are put into 6 closed-shell MOs ($4a_1$, $1b_1$ and $1b_2$), i.e., 1-4σ and 1π MOs.

To obtain more accurate PECs, potential energy is extrapolated to the complete basis set (CBS) limit with the aug-cc-pV5Z (AV5Z) and aug-cc-pV6Z (AV6Z) basis sets of Dunning [38,51,52], denoted as "56". Extrapolation formulas used here are given by Truhlar [53]

$$E_X^{ref} = E_\infty^{ref} + A^{ref}X^{-\alpha} \tag{1}$$

$$E_X^{cor} = E_\infty^{cor} + A^{cor}X^{-\beta} \tag{2}$$

where E_X^{ref} and E_X^{cor} are the reference and correlation energies, respectively, computed by the AVXZ basis set (here $X = 5$ and 6). E_∞^{ref} and E_∞^{cor} are the reference and correlation energies, respectively, determined by the CBS extrapolation. Extrapolation parameters α and β are given by Truhlar [53]. Core valence (CV) correlation energy correction is obtained by the icMRCI technique using the cc-pCV5Z basis set [38]. Scalar relativistic energy correction is calculated via third-order Douglas-Kroll-Hess (DKH3) Hamiltonian approximation [54,55] at the icMRCI/cc-pV5Z-DK [56] level of theory. Finally, PECs are obtained by the icMRCI+Q/56+CV+DK method.

TDMs are calculated by the valence icMRCI approach with the AV6Z basis set, as implemented in the MOLPRO 2015 program suite. The obtained PECs and TDMs are used to compute the radiative transition probabilities for dipole-allowed transitions of PN. Radiative lifetimes of vibrational levels for some electronic states of PN are also evaluated. Such transition parameters will be elaborated below.

2.3. Transition probabilities

Transition probabilities such as Einstein coefficients $A_{\upsilon'\upsilon''}$ and Franck-Condon factors $q_{\upsilon'\upsilon''}$ between an initial vibrational level υ' in the upper electronic state and a final vibrational level υ'' in the lower electronic state are as follows [57,58]

$$A_{\upsilon'\upsilon''} = 2.026 \times 10^{-6}\sigma_{\upsilon'\upsilon''}^3 \frac{2 - \delta_{0,\Lambda'+\Lambda''}}{2 - \delta_{0,\Lambda'}} \left(R_e^{\upsilon'\upsilon''}\right)^2 \tag{3}$$

$$q_{\upsilon'\upsilon''} = \left(\int \psi_{\upsilon'}(r)\psi_{\upsilon''}(r)dr\right)^2 \tag{4}$$

where $\sigma_{\upsilon'\upsilon''}$ is the wavenumber of a transition system, Λ' and Λ'' are the projections of electronic orbital angular momentum on the internuclear axis for the upper and lower electronic levels, respectively. $\psi_{\upsilon'}(r)$ and $\psi_{\upsilon''}(r)$ are the vibrational wave functions in the upper electronic state and those in the lower electronic state, respectively. $(R_e^{\upsilon'\upsilon'})$ is the square of electronic-vibrational transition

Table 1
Dissociation relationships of the 54 electronic states generated from the first six dissociation limits of PN.

Dissociation limit	Electronic state	Relative energy (cm^{-1})	
		This work[a]	Expt. [45]
$P(^4S_u)+N(^4S_u)$	$X^1\Sigma^+$, $a^3\Sigma^+$, $1^5\Sigma^+$, $1^7\Sigma^+$	0.00	0.00
$P(^4D_u)+N(^4S_u)$	$2^3\Sigma^+$, $b^3\Pi$, $d^3\Delta$, $2^5\Sigma^+$, $1^5\Pi$, $1^5\Delta$	11,415.49	11,368.83
$P(^2P_u)+N(^4S_u)$	$e^3\Sigma^-$, $2^3\Pi$, $1^5\Sigma^-$, $2^5\Pi$	18,577.95	18,735.36
$P(^4S_u)+N(^2D_u)$	$3^3\Sigma^+$, $3^3\Pi$, $2^3\Delta$, $3^5\Sigma^+$, $3^5\Pi$, $2^5\Delta$	19,097.32	19,228.82
$P(^4S_u)+N(^2P_u)$	$2^3\Sigma^-$, $4^3\Pi$, $2^5\Sigma^-$, $4^5\Pi$	28,780.23	28,839.11
$P(^2D_u)+N(^2D_u)$	$2^1\Sigma^+$, $3^1\Sigma^+$, $4^1\Sigma^+$, $C^1\Sigma^-$, $2^1\Sigma^-$, $A^1\Pi$, $2^1\Pi$, $3^1\Pi$, $4^1\Pi$, $D^1\Delta$, $2^1\Delta$, $3^1\Delta$, $1^1\Phi$, $2^1\Phi$, $1^1\Gamma$, $2^3\Sigma^+$, $3^3\Sigma^+$, $4^3\Sigma^+$, $C^3\Sigma^-$, $2^3\Sigma^-$, $A^3\Pi$, $2^3\Pi$, $3^3\Pi$, $4^3\Pi$, $D^3\Delta$, $2^3\Delta$, $3^3\Delta$, $1^3\Phi$, $2^3\Phi$, $1^3\Gamma$	30,174.01	30,104.19

[a] Obtained by the icMRCI+Q/56+CV+DK calculations.

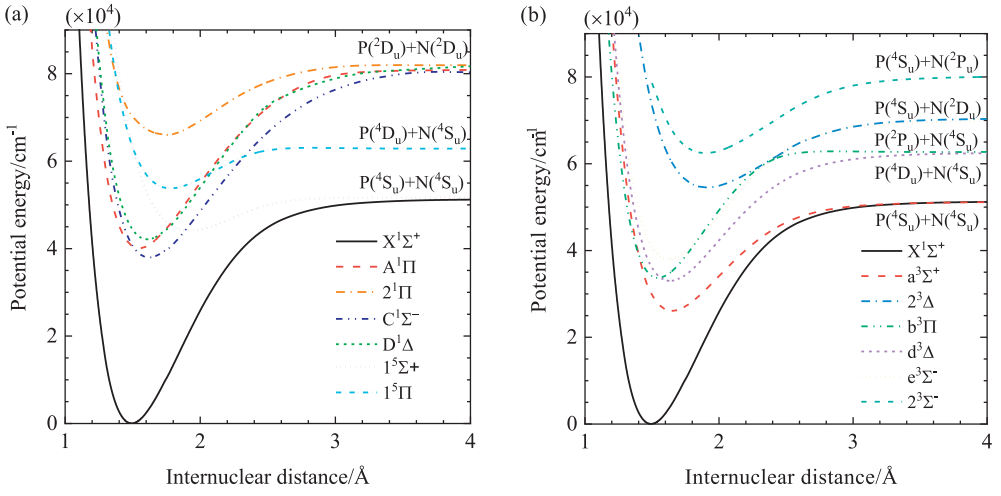

Fig. 1. PECs of **(a)** the $X^1\Sigma^+$, $A^1\Pi$, $C^1\Sigma^-$, $D^1\Delta$, $2^1\Pi$, $1^5\Sigma^+$ and $1^5\Pi$ electronic states **(b)** the $a^3\Sigma^+$, $b^3\Pi$, $d^3\Delta$, $e^3\Sigma^-$, $2^3\Delta$ and $2^3\Sigma^-$electronic states for PN calculated at the icMRCI+Q/56+CV+DK level of theory. The PECs are presented relative to the minimum of the ground state.

moment, which can be expressed in terms of wave function and TDM [58]

$$\left(R_e^{\upsilon'\upsilon''}\right)^2 = \left[\int_0^\infty \psi_{\upsilon'}(r) R_e(r) \psi_{\upsilon''}(r) dr\right]^2 \tag{5}$$

where $R_e(r)$ is the TDM. The total Einstein coefficients of a certain vibrational level υ' in the upper electronic state are obtained by summing the Einstein coefficients from this level to all possible vibrational levels υ'' in the lower electronic state. The radiative lifetimes of this level can be obtained by the reciprocal of the total Einstein coefficients

$$\tau_{\upsilon'} = \frac{1}{\sum_{\upsilon''=0}^{\upsilon''_{\max}} A_{\upsilon'\upsilon''}} \tag{6}$$

where $\tau_{\upsilon'}$ is radiative lifetimes of vibrational level υ'.

3. Results and discussion

The PECs of the $X^1\Sigma^+$, $A^1\Pi$, $C^1\Sigma^-$, $D^1\Delta$, $2^1\Pi$, $a^3\Sigma^+$, $b^3\Pi$, $d^3\Delta$, $e^3\Sigma^-$, $2^3\Delta$, $2^3\Sigma^-$, $1^5\Sigma^+$ and $1^5\Pi$ electronic states for PN are calculated at the icMRCI+Q/56+CV+DK level of theory and shown in Fig. 1. Figs. 2 and 3 present the TDMs of 15 band transition systems. The obtained PECs are involved in the LEVEL program [59] to calculate the spectroscopic parameters (Table 2). Specifically speaking, the vibrational levels G_υ and internal rotation constant B_υ are first determined by solving the nuclear radial Schrödinger equation over the PECs. The spectroscopic parameters of each state are then fitted by its G_υ and B_υ values, which are given in the Appendix for determining the vibrational band origins. The spectral regions of strong emissions for 15 band systems are presented in Table 3.

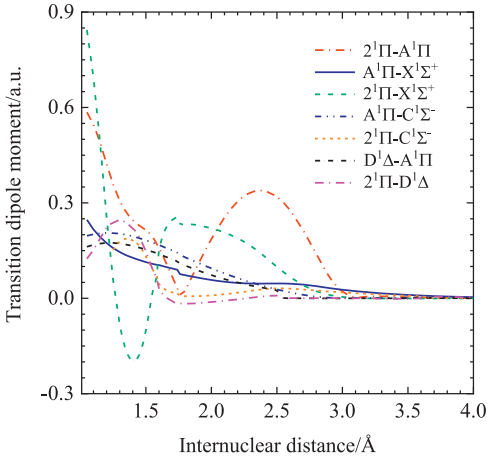

Fig. 2. Curves of TDM versus internuclear distance for seven band transition systems between five singlet states.

In order to clearly understand the electronic transitions between different states, the dominant valence electron configurations of each state near the equilibrium internuclear distance are calculated at the icMRCI/AV6Z level of theory and listed in Table 4. Using the PECs and TDMs obtained here, we compute the radiative transition probabilities for 15 dipole allowed transitions. Some relatively large Einstein coefficients and Franck-Condon factors are listed in Tables 5–10. The radiative lifetimes of some excited states are also determined from the obtained Einstein coefficients and are given in Table 11. From the selection rules of electric dipole tran-

Table 2
Spectroscopic parameters of 13 electronic states for PN calculated at the icMRCI+Q/56+CV+DK level of theory.

State		D_e/cm^{-1}	T_e/cm^{-1}	R_e/Å	ω_e/cm^{-1}	$\omega_e\chi_e$/cm^{-1}	$10^2\omega_e y_e$/cm^{-1}	B_e/cm^{-1}	$10^3\alpha_e$/cm^{-1}
$X^1\Sigma^+$	This work	51,454.07	0.00	1.4918	1339.61	6.594	−8.202	0.78549	5.29
	Expt. [13]	50,812.91	0.00	1.4869	1337.24	6.983		0.78621	5.57
	Expt. [60]		0.00	1.49086	1335.6	6.5		0.786489	
	Expt. [19]		0.00	1.49105	1336.98	6.906		0.78628	5.31
	Expt. [20]		0.00		1337.0	6.88	0.7	0.786486	5.538
	Expt. [21]		0.00	1.491	1337.0	6.88		0.78648	5.54
	Expt. [24]		0.00		1336.948	6.8958		0.7864844	5.5337
	Expt. [27]	51,938.86[a]	0.00		1336.9992	6.9164	−0.352	0.78648	5.554
	Calc. [31]	44,279.82	0.00	1.488	1400.6	9.33		0.789	6.6
	Calc. [39]	50,479.80	0.00	1.4894	1351.30				
	Calc. [40]	51,108.67[b]	0.00	1.4968	1336.2	6.6		0.7803	5.27
	Calc. [42]	45,973.58	0.00	1.552	1363.5				
	Calc. [27]	51,287.97	0.00	1.4894	1352.2	6.58		0.788412	5.363
	Calc. [61]	50,645.15	0.00	1.4948	1333.84	6.83729		0.78230	5.44
	Calc. [44][c]	49,683.73	0.00	1.4977	1328.21	5.7768	2.029	0.77872	5.8
$A^1\Pi$	This work	40,995.53	40,032.55	1.5476	1104.81	7.520	35.019	0.73060	7.47
	Expt. [13]	41,134.26	39,688.52	1.5424	1103.09	7.222		0.73071	6.63
	Expt. [20]		39,805.9		1103.0	7.25		0.7310	6.41
	Expt. [21]		39,805.64	1.547	1103.0	7.25		0.7310	6.40
	Calc. [31]	35,085.10	40,327.71	1.566	1071.7	11.4		0.713	7.5
	Calc. [37]		40,007.6	1.5732	1066.3	10.72		0.7063	1.83
	Calc. [61]	41,331.86		1.5501	1100.24	7.21846		0.727505	6.33
	Calc. [44][c]	40,624.26	40,610.00	1.556	1078.42	7.3099	11.315	0.72130	4.9
$D^1\Delta$	This work	39,993.49	42,106.86	1.6073	1018.98	7.527	21.132	0.67724	5.9
	Calc. [31]	33,713.96	41,618.19	1.622	967.9	1.97		0.664	7.0
	Calc. [37]		40,345.5	1.6252	1105.7	16.17		0.6619	2.98
	Calc. [61]	41,555.28		1.6196	1002.269	4.28833		0.665056	2.81
	Calc. [44][c]	39,488.89	41,835.96	1.614	1010.647	1.5168	33.974	0.671	5.3
$C^1\Sigma^-$	This work	42,766.02	39,298.72	1.6211	977.5	4.9329	5.88	0.66390	5.72
	Calc. [31]	37,827.38	37,504.77	1.617	1108.8	8.70		0.669	5.1
	Calc. [44][c]	41,852.09	39,505.02	1.627	973.927	2.7984	114.483	0.6597	5.5
$2^1\Pi$	This work	16,044.34	65,916.71	1.7650	733.20	17.515	71.498	0.7306	7.47
	Calc. [31]		70,170.21						
	Calc. [44][d]	15,526.17	65,742.22	1.730	648.93	9.8953	132.984	0.5833	6.1
$a^3\Sigma^+$	This work	25,249.32	26,065.66	1.6481	941.61	8.742	10.967	0.64253	5.47
	Calc. [31]	19,599.26	24,761.21	1.669	787.4	10.09		0.628	1.10
	Calc. [44][c]	23,785.28	25,817.80	1.655	913.765	3.8056	43.011	0.6375	6.9
$b^3\Pi$	This work	29,197.77	33,671.79	1.5449	1113.24	2.940	31.621	0.73301	7.34
	Calc. [31]	21,696.31	34,359.20	1.558	1124.3	9.94		0.720	7.2
	Calc. [44][d]	27,672.87	33,843.01	1.555	1102.494	8.4532	10.777	0.7224	5.1
$d^3\Delta$	This work	29,679.37	32,975.56	1.6324	949.99	4.599	0.825	0.65376	4.81
	Calc. [31]	23,551.38	32,504.13	1.666	770.3	−14.51		0.629	6.0
	Calc. [44][c]	28,471.36	33,125.18	1.640	959.263	5.3371	22.199	0.6495	6.9
$e^3\Sigma^-$	This work	32,081.01	37,951.02	1.6240	981.37	5.828	2.847	0.66149	4.77
	Calc. [31]	37,827.39	37,504.77	1.617	1108.8	9.70		0.669	5.1
	Calc. [44][c]	30,665.19	37,956.44	1.632	982.255	6.7247	4.224	0.6556	6.9
$2^3\Delta$	This work	16,047.04	54,504.35	1.9089	622.74	3.570	2.387	0.47988	4.23
	Calc. [44][d]	14,759.94	54,232.70	1.918	607.601	4.1129	8.777	0.4747	4.4
$2^3\Sigma^-$	This work	17,798.26	62,436.04	1.9002	631.87	3.289	2.808	0.48405	3.99
	Calc. [44][d]	16,445.64	61,911.09	1.909	616.566	5.0133	27.685	0.4794	4.1
$1^5\Sigma^+$	This work	7717.77	44,095.84	1.9237	572.41	1.223	33.983	0.47058	3.65
	Calc. [44][d]	6226.60	43,263.56	1.927	565.348	8.4164	7.756	0.4703	5.3
$1^5\Pi$	This work	9303.92	53,760.81	1.7802	703.86	9.155	12.030	0.55130	4.97
	Calc. [44][d]	8444.62	53,039.00	1.784	711.832	13.8384	77.754	0.5486	6.7

[a] Obtained from the experimental D_0 at T = 0 K [28], and the experimental vibrational correction [27].
[b] Obtained from thetheoretical D_0 [40] and the zero point energy in this work.
[c] Obtained by MRCI/AV(5+d)Z level of theory.
[d] Obtained by MRCI/AV5Z level of theory.

Table 3
Spectral regions of the strong emissions for 15 band systems.

Band system	Spectral region	Band system	Spectral region	Band system	Spectral region
$A^1\Pi$-$X^1\Sigma^+$	UV[a]	$2^1\Pi$-$C^1\Sigma^-$	UV and visible	$2^3\Delta$-$b^3\Pi$	UV
$A^1\Pi$-$C^1\Sigma^-$	Infrared	$2^1\Pi$-$D^1\Delta$	UV and visible	$2^3\Delta$–$1^3\Delta$	UV to mid-infrared
$D^1\Delta$-$A^1\Pi$	Near-infrared	$b^3\Pi$-$a^3\Sigma^+$	Visible and near-infrared	$2^3\Sigma^-$–$1^3\Sigma^-$	UV to infrared
$2^1\Pi$-$A^1\Pi$	UV to far-infrared	$b^3\Pi$-$d^3\Delta$	Mid-infrared	$2^3\Sigma^-$-$b^3\Pi$	UV
$2^1\Pi$-$X^1\Sigma^+$	UV and visible	$e^3\Sigma^-$-$b^3\Pi$	Near- and Mid-infrared	$1^5\Pi$–$1^5\Sigma^+$	VUV[b]

[a] UV is the abbreviation of ultraviolet.
[b] VUV is the abbreviation of vacuum ultraviolet.

Table 4
Dominant electron configurations of 13 electronic states for PN near their corresponding equilibrium internuclear distances.

State	Main electron configuration	State	Main electron configuration	State	Main electron configuration
$X^1\Sigma^+$	$5\sigma^2 6\sigma^2 2\pi^4 7\sigma^2 3\pi^0 8\sigma^0$(0.899)[a]	$a^3\Sigma^+$	$5\sigma^2 6\sigma^2 2\pi^3 7\sigma^2 3\pi^1 8\sigma^0$(0.645)	$2^3\Delta$	$5\sigma^2 6\sigma^2 2\pi^2 7\sigma^2 3\pi^2 8\sigma^0$(0.758)
$A^1\Pi$	$5\sigma^2 6\sigma^2 2\pi^4 7\sigma^1 3\pi^1 8\sigma^0$(0.890)		$5\sigma^2 6\sigma^2 2\pi^1 7\sigma^2 3\pi^3 8\sigma^0$(0.148)	$2^3\Sigma^-$	$5\sigma^2 6\sigma^2 2\pi^2 7\sigma^2 3\pi^2 8\sigma^0$(0.905)
$C^1\Sigma^-$	$5\sigma^2 6\sigma^2 2\pi^3 7\sigma^2 3\pi^1 8\sigma^0$(0.657)	$d^3\Delta$	$5\sigma^2 6\sigma^2 2\pi^3 7\sigma^2 3\pi^1 8\sigma^0$(0.899)	$1^5\Sigma^+$	$5\sigma^2 6\sigma^2 2\pi^2 7\sigma^2 3\pi^2 8\sigma^0$(0.930)
$D^1\Delta$	$5\sigma^2 6\sigma^2 2\pi^3 7\sigma^2 3\pi^1 8\sigma^0$(0.654)		$5\sigma^2 6\sigma^2 2\pi^1 7\sigma^2 3\pi^3 8\sigma^0$(0.114)	$1^5\Pi$	$5\sigma^2 6\sigma^2 2\pi^3 7\sigma^1 3\pi^2 8\sigma^0$(0.930)
$2^1\Pi$	$5\sigma^2 6\sigma^2 2\pi^3 7\sigma^1 3\pi^2 8\sigma^0$(0.593)	$b^3\Pi$	$5\sigma^2 6\sigma^2 2\pi^4 7\sigma^1 3\pi^1 8\sigma^0$(0.903)		
	$5\sigma^2 6\sigma^2 2\pi^3 7\sigma^2 3\pi^0 8\sigma^1$(0.185)	$e^3\Sigma^-$	$5\sigma^2 6\sigma^2 2\pi^3 7\sigma^2 3\pi^1 8\sigma^0$(0.648)		

The coefficients lower than 0.1 are not given here. Core configuration of each electronic state is $1\sigma^2 2\sigma^2 3\sigma^2 4\sigma^2 1\pi^4$.
[a] Values in parentheses are the coefficients squared of configuration state function (CSF) which are relevant to the electron configuration.

Table 5
Einstein coefficients (s^{-1}) and Franck-Condon factors of the $A^1\Pi$-$X^1\Sigma^+$, $A^1\Pi$-$C^1\Sigma^-$, $D^1\Delta$-$A^1\Pi$ and $2^1\Pi$-$A^1\Pi$ systems for PN.

$A^1\Pi$-$X^1\Sigma^+$			$A^1\Pi$-$C^1\Sigma^-$			$D^1\Delta$-$A^1\Pi$			$2^1\Pi$-$A^1\Pi$		
υ'-υ''	EC[a]	FC[b]	υ'-υ''	EC	FC	υ'-υ''	EC	FC	υ'-υ''	EC	FC
0–0	9.10E+05	0.5577	1–0	3.46E+02	0.3849	1–0	7.52E+02	0.2759	0–1	1.80E+04	0.0542
0–1	4.16E+05	0.3179	2–0	4.46E+02	0.1248	2–0	7.73E+02	0.0903	0–2	1.93E+04	0.1221
1–0	6.26E+05	0.3105	3–1	9.97E+02	0.2458	3–1	1.45E+03	0.1584	0–3	1.13E+04	0.1862
1–1	1.68E+05	0.0995	4–1	5.29E+02	0.0619	4–1	1.47E+03	0.0700	1–0	6.58E+04	0.0712
1–2	4.36E+05	0.3287	4–2	1.43E+03	0.3158	4–2	1.86E+03	0.1798	1–1	9.13E+04	0.1690
1–3	2.01E+05	0.1847	5–2	1.12E+03	0.1251	5–2	2.37E+03	0.1050	1–2	4.73E+04	0.1683
2–0	2.31E+05	0.0924	5–3	1.55E+03	0.3134	5–3	1.74E+03	0.1542	2–0	1.87E+05	0.1392
2–1	6.21E+05	0.3067	6–3	1.64E+03	0.2077	6–2	1.86E+03	0.0449	2–1	1.20E+05	0.1429
2–3	2.90E+05	0.2174	6–4	1.51E+03	0.2755	6–3	2.89E+03	0.1213	2–2	1.10E+04	0.0224
2–4	2.64E+05	0.2423	7–4	2.09E+03	0.2077	6–4	1.32E+03	0.1070	3–0	3.90E+05	0.2075
3–1	4.53E+05	0.1826	7–5	1.37E+03	0.2281	7–2	1.16E+03	0.0171	3–1	6.54E+04	0.0518
3–2	3.88E+05	0.1884	8–5	2.78E+03	0.2612	7–3	2.95E+03	0.0681	3–2	1.47E+04	0.0212
3–4	1.28E+05	0.0958	8–6	1.11E+03	0.1718	7–4	3.08E+03	0.1230	4–0	5.01E+05	0.1973
3–5	2.69E+05	0.2461	9–6	3.21E+03	0.2868	8–3	2.05E+03	0.0293	4–2	9.49E+04	0.0880
3–6	1.33E+05	0.1485	10–6	1.13E+03	0.0810	8–4	3.64E+03	0.0809	4–3	1.99E+04	0.0292
4–1	1.84E+05	0.0598	10–7	3.62E+03	0.3063	8–5	2.86E+03	0.1073	5–0	5.43E+05	0.1626
4–2	5.42E+05	0.2193	11–7	1.51E+03	0.1055	9–3	1.21E+03	0.0116	5–1	1.01E+05	0.0459
4–3	1.46E+05	0.0696	11–8	3.99E+03	0.3240	9–5	4.12E+03	0.0891	5–2	1.10E+05	0.0701
4–4	1.91E+05	0.1186	12–8	1.84E+03	0.1261	9–6	2.66E+03	0.0929	5–4	3.78E+04	0.0721
4–6	2.22E+05	0.2031	12–9	4.17E+03	0.3233	10–4	2.00E+03	0.0186	6–0	4.39E+05	0.1027
4–7	1.70E+05	0.1917	13–9	2.25E+03	0.1506	10–5	3.95E+03	0.0526	6–1	3.43E+05	0.1152

[a] EC refers to Einstein coefficient.
[b] FC is denoted as Franck-Condon factor.

Table 6
Einstein coefficients (s^{-1}) and Franck-Condon factors of the $2^1\Pi$-$X^1\Sigma^+$, $2^1\Pi$-$C^1\Sigma^-$ and $2^1\Pi$-$D^1\Delta$ systems for PN.

$2^1\Pi$-$X^1\Sigma^+$			$2^1\Pi$-$C^1\Sigma^-$			$2^1\Pi$-$D^1\Delta$		
υ'-υ''	EC[a]	FC[b]	υ'-υ''	EC	FC	υ'-υ''	EC	FC
0–2	1.73E+05	0.0103	1–0	1.90E+04	0.0040	2–0	1.07E+04	0.2819
0–3	5.84E+05	0.0271	2–0	2.84E+04	0.0148	3–0	2.65E+04	0.1768
0–4	1.32E+06	0.0545	3–0	3.35E+04	0.0416	3–1	1.36E+04	0.1561
0–5	2.20E+06	0.0891	3–1	3.97E+04	0.1044	4–0	3.37E+04	0.0635
0–6	2.93E+06	0.1226	4–0	2.58E+04	0.0748	4–1	3.68E+04	0.2199
0–7	3.32E+06	0.1464	4–1	6.17E+04	0.1116	4–2	1.02E+04	0.0210
0–8	3.23E+06	0.1538	4–2	2.77E+04	0.0438	5–0	3.10E+04	0.0160
0–9	2.57E+06	0.1385	5–0	1.66E+04	0.1182	5–1	6.57E+04	0.1529
0–10	1.62E+06	0.1031	5–1	6.32E+04	0.0866	5–2	3.30E+04	0.1626
1–3	2.26E+06	0.1033	5–2	7.20E+04	0.0019	6–0	1.79E+04	0.0020
1–4	3.35E+06	0.1274	5–3	1.84E+04	0.0361	6–1	6.85E+04	0.0572
1–5	3.02E+06	0.1094	6–1	4.16E+04	0.0353	6–2	6.81E+04	0.1914
1–6	1.57E+06	0.0587	6–2	8.64E+04	0.0150	6–3	2.68E+04	0.0739
1–10	1.52E+06	0.0793	6–3	6.38E+04	0.0607	7–1	4.69E+04	0.0115
2–2	1.36E+06	0.0999	6–4	1.16E+04	0.0138	7–2	9.41E+04	0.1094
2–3	2.24E+06	0.1000	7–1	1.84E+04	0.0025	7–3	6.82E+04	0.1841
2–4	1.58E+06	0.0505	7–2	6.50E+04	0.0553	7–4	2.59E+04	0.0170
2–5	1.99E+05	0.0044	7–3	1.06E+05	0.0331	8–1	1.97E+04	0.0007
2–6	2.98E+05	0.0108	7–4	5.94E+04	0.0042	8–2	8.39E+04	0.0335
2–7	1.47E+06	0.0530	8–2	3.23E+04	0.0680	8–3	1.11E+05	0.1531
2–8	1.78E+06	0.0738	8–3	1.01E+05	0.0016	8–4	6.64E+04	0.1428

[a] EC refers to Einstein coefficient.
[b] FC is denoted as Franck-Condon factor.

Table 7
Spectroscopic parameters of the $b^3\Pi$ and $e^3\Sigma^-$ electronic states for PN obtained by fitting the calculated energy levels approximately lying at $\upsilon = 0$–4 levels of the $A^1\Pi$ state.

State		D_e/cm^{-1}	T_e/cm^{-1}	R_e/Å	ω_e/cm^{-1}	$\omega_e\chi_e$/cm^{-1}	$10^2\omega_e y_e$/cm^{-1}	B_e/cm^{-1}	$10^3\alpha_e$/cm^{-1}
$b^3\Pi$	This work	29,197.77	33,671.79	1.5449	1137.10	8.556		0.73246	6.57
	Expt. [21]		33,370.00	1.497	1150.0	8.00		0.78	5.00
$e^3\Sigma^-$	This work	32,081.01	37,951.02	1.6240	981.37	5.828	2.847	0.66149	4.77
	Expt. [21]		37,330.00	1.637	992.0	5.00		0.6525	5.00

Table 8
Einstein coefficients (s^{-1}) and Franck-Condon factors of the $b^3\Pi$-$a^3\Sigma^+$, $b^3\Pi$-$d^3\Delta$, $e^3\Sigma^-$-$b^3\Pi$ and $2^3\Delta$-$b^3\Pi$ systems for PN.

$b^3\Pi$-$a^3\Sigma^+$			$b^3\Pi$-$d^3\Delta$			$e^3\Sigma^-$-$b^3\Pi$			$2^3\Delta$-$b^3\Pi$		
υ'-υ''	EC[a]	FC[b]	υ'-υ''	EC	FC	υ'-υ''	EC	FC	υ'-υ''	EC	FC
0–0	9.45E+03	0.2046	1–0	4.24E+02	0.3953	0–0	3.70E+03	0.3846	3–4	1.20E+01	0.0443
0–1	7.29E+03	0.2815	2–0	9.36E+02	0.2067	0–1	1.07E+03	0.3964	3–5	1.40E+01	0.0736
0–2	2.85E+03	0.2275	2–1	2.47E+02	0.1790	1–0	9.03E+03	0.3261	4–3	1.50E+01	0.0313
1–0	2.91E+04	0.3616	3–0	6.38E+02	0.0579	2–0	1.04E+04	0.1703	4–4	2.20E+01	0.0617
1–1	3.38E+03	0.0652	3–1	1.51E+03	0.2930	2–1	4.72E+03	0.1545	4–5	1.90E+01	0.0695
2–0	3.40E+04	0.2723	4–0	1.92E+02	0.0095	3–0	7.94E+03	0.0688	5–2	1.40E+01	0.0177
2–1	4.70E+03	0.0555	4–1	1.74E+03	0.1464	3–1	1.30E+04	0.1987	5–3	2.90E+01	0.0466
2–2	9.29E+03	0.1656	4–2	1.42E+03	0.2447	3–3	2.32E+03	0.1494	5–4	3.20E+01	0.0672
2–3	1.29E+03	0.0377	5–1	7.63E+02	0.0360	4–0	4.64E+03	0.0237	5–5	1.60E+01	0.0445
3–0	2.00E+04	0.1128	5–2	2.77E+03	0.2170	4–1	1.57E+04	0.1300	6–2	2.90E+01	0.0282
3–1	3.33E+04	0.2560	5–3	9.89E+02	0.1524	4–2	9.20E+03	0.1318	6–3	4.60E+01	0.0579
3–3	5.47E+03	0.0903	6–1	1.62E+02	0.0051	4–4	2.76E+03	0.1555	6–4	3.50E+01	0.0566
3–4	3.96E+03	0.1041	6–2	1.61E+03	0.0732	5–0	2.31E+03	0.0075	7–1	1.90E+01	0.0118
4–0	6.58E+03	0.0279	6–3	3.37E+03	0.2471	5–1	1.28E+04	0.0632	7–2	4.90E+01	0.0391
4–1	4.01E+04	0.2198	6–4	4.99E+02	0.0704	5–2	1.84E+04	0.1454	7–3	6.00E+01	0.0607
4–2	1.56E+04	0.1156	6–5	3.22E+02	0.0977	5–3	4.17E+03	0.0567	7–4	2.70E+01	0.0352
4–3	8.47E+03	0.0853	7–2	3.83E+02	0.0120	5–4	1.52E+03	0.0362	7–7	1.30E+01	0.0379
4–5	4.16E+03	0.0987	7–3	2.54E+03	0.1115	5–5	2.34E+03	0.1163	8–1	3.50E+01	0.0180
4–6	1.53E+03	0.0610	7–4	3.62E+03	0.2494	6–0	1.02E+03	0.0022	8–2	7.40E+01	0.0483
5–0	1.29E+03	0.0045	7–5	1.23E+02	0.0166	6–1	8.03E+03	0.0256	8–3	6.50E+01	0.0538
5–1	2.04E+04	0.0851	7–6	4.67E+02	0.1205	6–2	2.01E+04	0.0966	8–4	1.30E+01	0.0138
5–2	4.65E+04	0.2484	8–3	7.19E+02	0.0223	6–3	1.59E+04	0.1203	9–0	1.20E+01	0.0041
5–3	2.56E+03	0.0189	8–4	3.77E+03	0.1597	6–5	3.43E+03	0.0756	9–1	5.80E+01	0.0250
5–6	2.26E+03	0.0486	8–5	3.45E+03	0.2245	6–6	1.47E+03	0.0653	9–2	9.90E+01	0.0533
5–7	2.36E+03	0.0824	8–7	5.10E+02	0.1129	7–1	4.29E+03	0.0093	9–3	5.80E+01	0.0395

[a] EC refers to Einstein coefficient.
[b] FC is denoted as Franck-Condon factor.

Table 9
Einstein coefficients (s^{-1}) and Franck-Condon factors of the $2^3\Delta$–$1^3\Delta$, $2^3\Sigma^-$–$1^3\Sigma^-$ and $2^3\Sigma^-$-$b^3\Pi$ systems for PN.

$2^3\Delta$-$1^3\Delta$			$2^3\Sigma^-$-$1^3\Sigma^-$			$2^3\Sigma^-$-$b^3\Pi$		
υ'-υ''	EC[a]	FC[b]	υ'-υ''	EC	FC	υ'-υ''	EC	FC
0–3	1.52E+03	0.0397	0–3	2.82E+03	0.0354	5–3	1.13E+03	0.0597
0–4	2.70E+03	0.0883	0–4	5.41E+03	0.0797	6–2	1.53E+03	0.0404
0–5	3.47E+03	0.1426	0–5	7.62E+03	0.1340	6–3	1.71E+03	0.0665
0–6	3.47E+03	0.1814	0–6	8.38E+03	0.1764	7–1	1.34E+03	0.0190
1–2	2.93E+03	0.0484	0–7	7.36E+03	0.1853	7–2	2.52E+03	0.0516
1–3	4.81E+03	0.0968	0–8	5.18E+03	0.1568	7–3	2.05E+03	0.0599
1–4	5.13E+03	0.1266	0–9	2.89E+03	0.1062	8–1	2.43E+03	0.0274
2–1	3.23E+03	0.0354	1–2	4.77E+03	0.0435	8–2	3.57E+03	0.0579
2–2	6.67E+03	0.0878	1–3	9.12E+03	0.0922	8–3	1.92E+03	0.0435
2–3	6.66E+03	0.1056	1–4	1.07E+04	0.1249	9–0	1.21E+03	0.0074
3–1	6.93E+03	0.0624	1–5	7.18E+03	0.1002	9–1	4.01E+03	0.0363
3–2	9.45E+03	0.1010	2–1	4.30E+03	0.0325	9–2	4.41E+03	0.0579
3–3	4.46E+03	0.0571	2–2	1.07E+04	0.0831	9–3	1.31E+03	0.0238
3–6	3.35E+03	0.0725	2–3	1.31E+04	0.1079	10–0	2.27E+03	0.0111
4–0	3.73E+03	0.0238	2–4	7.02E+03	0.0649	10–1	6.07E+03	0.0446
4–1	1.11E+04	0.0832	2–7	5.35E+03	0.0794	10–2	4.75E+03	0.0515
4–2	8.92E+03	0.0788	2–8	4.27E+03	0.0768	11–0	4.00E+03	0.0158
4–5	4.35E+03	0.0626	3–1	8.81E+03	0.0604	11–1	8.49E+03	0.0511
5–0	7.00E+03	0.0379	3–2	1.50E+04	0.1013	11–2	4.36E+03	0.0402
5–1	1.45E+04	0.0913	3–3	9.53E+03	0.0637	12–0	6.61E+03	0.0211
5–2	5.46E+03	0.0404	4–0	3.66E+03	0.0245	12–1	1.10E+04	0.0545
5–4	5.39E+03	0.0538	4–1	1.29E+04	0.0831	12–2	3.26E+03	0.0263
5–5	2.54E+03	0.0301	4–2	1.34E+04	0.0816	12–4	2.57E+03	0.0332
5–7	3.16E+03	0.0506	4–5	8.44E+03	0.0624	13–0	1.03E+04	0.0268
6–0	1.14E+04	0.0529	4–8	5.52E+03	0.0565	13–1	1.31E+04	0.0539

[a] EC refers to Einstein coefficient.
[b] FC is denoted as Franck-Condon factor.

Table 10
Einstein coefficients (s^{-1}) and Franck-Condon factors of the $1^5\Pi$-$1^5\Sigma^+$ system for PN.

υ'-υ''	EC[a]	FC[b]	υ'-υ''	EC	FC	υ'-υ''	EC	FC	υ'-υ''	EC	FC
0–0	1.95E+04	0.1425	0–1	2.20E+04	0.2395	0–2	1.30E+04	0.2305	1–0	6.51E+04	0.3247
1–1	1.78E+04	0.1181	2–0	8.41E+04	0.3157	2–2	2.25E+04	0.1418	3–0	8.41E+04	0.3157
3–1	6.12E+04	0.2389	3–4	1.19E+04	0.0972	4–0	1.13E+04	0.0361	4–1	7.84E+04	0.2554
4–2	2.13E+04	0.0857	4–3	2.53E+04	0.1094	5–1	3.10E+04	0.0980	5–2	8.23E+04	0.2671
5–4	2.80E+04	0.1202	6–2	5.71E+04	0.1778	6–3	6.59E+04	0.2193	6–5	1.64E+04	0.0711
6–6	1.41E+04	0.0692	7–2	1.17E+04	0.0433	7–3	7.50E+04	0.2399	7–4	3.98E+04	0.1382
7–5	1.75E+04	0.0535	7–7	1.57E+04	0.0759	8–3	1.95E+04	0.0747	8–4	8.67E+04	0.2830

[a] EC refers to Einstein coefficient.
[b] FC is denoted as Franck-Condon factor.

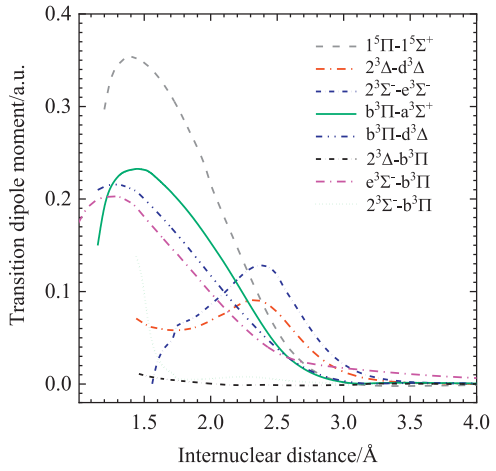

Fig. 3. Curves of TDM versus internuclear distance for eight band transition systems between six triplet states or two quintet states.

Table 11
Radiative lifetimes of the first 15 vibrational levels for the $A^1\Pi$, $D^1\Delta$, $2^1\Pi$, $b^3\Pi$, $e^3\Sigma^-$, $2^3\Delta$, $2^3\Sigma^-$ and $1^5\Pi$ states of PN.

υ'	$A^1\Pi$ τ/ns	$D^1\Delta$ τ/μs	$2^1\Pi$ τ/ns	$b^3\Pi$ τ/μs	$e^3\Sigma^-$ τ/μs	$2^3\Delta$ τ/μs	$2^3\Sigma^-$ τ/μs	$1^5\Pi$ τ/μs
0	659.4	3872	50.28	49.20	206.9	56.87	23.13	16.35
1	674.3	1186	50.63	27.81	98.46	42.93	18.85	10.81
2	660.8	615.2	55.99	19.50	59.45	33.60	15.71	8.249
3	646.5	378.3	60.61	15.05	40.75	26.10	12.70	6.854
4	642.2	246.8	64.90	12.40	30.41	19.23	9.848	6.288
5	643.0	181.8	64.24	10.62	23.68	15.34	8.406	5.817
6	632.1	144.3	61.68	9.364	19.26	13.10	7.440	5.606
7	610.6	113.0	57.68	8.356	16.16	10.95	6.371	5.695
8	607.4	95.96	55.38	7.458	13.93	9.566	5.574	5.237
9	598.6	79.54	52.45	6.881	12.20	8.340	4.864	4.950
10	583.8	69.81	49.10	6.232	10.77	7.358	4.289	5.576
11	581.8	60.17	47.20	5.592	9.517	6.637	3.875	5.678
12	566.8	53.86	45.59	5.283	8.146	5.947	3.457	5.111
13	565.3	45.02	44.30	4.819	7.142	5.412	3.116	6.056
14	553.1	37.37	43.37	4.303	6.192	4.991	2.839	7.613

sitions, radiative transition can only occur between the states with the same spin multiplicity. So all the electronic transitions considered here are discussed in three groups.

3.1. Radiative transitions between singlet states

The ground $X^1\Sigma^+$ state of PN mainly consists of the $5\sigma^2 6\sigma^2 2\pi^4 7\sigma^2 3\pi^0 8\sigma^0$ valence electron configuration around the equilibrium internuclear distance. Recent laboratory study of the $X^1\Sigma^+$ state was performed by Cazzoli et al. [27] using microwave spectroscopy. Accurate rovibrational spectroscopic constants were thus determined to be 1337.00, 6.9164, 0.78648 and 0.00554 cm^{-1} for ω_e, $\omega_e\chi_e$, B_e and α_e, respectively. Our calculated ω_e = 1339.61 cm^{-1}, $\omega_e\chi_e$ = 6.5943 cm^{-1}, B_e = 0.78621 cm^{-1} and α_e = 0.00571 cm^{-1} are in excellent agreement with the experimental data [27]. The determined R_e = 1.4918 Å is also much close to the experimental value, of which the deviation is only 0.0009 Å. The obtained dissociation energy D_e of 51,454.07 cm^{-1} agrees quite well with the theoretical value of 51,287.97 cm^{-1} and the experimental value of 51,938.86 cm^{-1} both obtained by Cazzoli et al. [27]. It is worth noting that the experimental value of D_e is derived from the experimental $D_0(P^{14}N)$ at T = 0 K [28] with the experimental vibrational correction [27].

The excited $A^1\Pi$ state has a potential well with D_e = 40,995.53 cm^{-1}, which is slightly lower than the experimentally determined value 41,134.26 cm^{-1} [15]. The electronic excitation energy T_e is determined to be 40,032.55 cm^{-1}. The discrepancy with the experimental result [20] is only 126.65 cm^{-1}. The calculated ω_e, $\omega_e\chi_e$, B_e and r_e are in good agreement with those reported from the experimental measurements [20,21] and an recent theoretical calculation [61], which confirms that this state is both reliable and accurate.

The TDMs of the $A^1\Pi$-$X^1\Sigma^+$ system are given in Fig. 2. Due to the non-orthogonality of the vibrational functions between these two states, large values of radiative transition probabilities locate near diagonal matrix elements. Some large Einstein coefficients and Franck-Condon factors of the $A^1\Pi$-$X^1\Sigma^+$ system are presented in Table 5.

As mentioned in the Introduction, the $A^1\Pi$-$X^1\Sigma^+$ system is one of the most important band systems of PN. Many emission bands of this system have been recorded and a number of vibrational band origins have been determined. Ghosh et al. [20] observed the emission spectrum of PN at high resolution in the 2200–3100 Å region and recorded thirty-six bands. The vibrational band origins of the 0–0, 0–1, 1–0, 1–2, 2–0, 2–1, 2–3, 3–1, 3–2, 4–2 and 4–3 bands were also reported by Saraswathy and Krishnamurty [21]. Our calculated vibrational band origins are in excellent agreement with the experimental data [20,21], e.g., the band origins of the 0–0, 0–1, 1–0, 1–2, 2–0, 2–3, 3–1, 3–2 and 4–2 bands are calculated to be 39,905.85 (2507.63 Å), 38,579.62 (2593.84 Å), 40,986.14 (2441.54 Å), 38,347.19 (2609.56 Å), 42,051.56 (2379.68 Å), 38,116.69 (2625.34 Å), 41,773.58 (2395.51 Å), 40,460.87 (2473.23 Å) and 41,485.30 (2412.16 Å), respectively. The corresponding experimental ones given by Ghosh et al. [20] are 39,688.55, 38,365.39, 40,777.13, 38,144.62, 41,850.53, 37,922.82, 41,589.34, 40,280.10 and 41,323.70, respectively. The vibrational band origins of these nine bands reported by Saraswathy and Krishnamurty [21] are 39,699.81 (2518.14 Å), 38,377.70 (2604.9 Å), 40,787.02 (2451.02 Å), 38,156.30 (2620.02 Å), 41,858.37 (2388.28 Å), 37,933.45 (2635.41 Å), 41,597.00 (2403.29 Å), 40,288.82 (2481.33 Å) and 41,330.98 (2418.76 Å), respectively. Moreover, the calculated vibrational band origins including υ' = 0–5 to υ''=0–4 transitions are in quite good agreement with previous theoretical results [37].

Relative transition probabilities of nine bands for the $A^1\Pi$-$X^1\Sigma^+$ system are obtained by Moeller and Silvers [17] from the

observed fluoresence and lamp intensities. Our calculated Franck-Condon factors of the 0–0, 0–1, 0–2, 0–3, 1–0, 1–1, 1–2, 1–3 and 1–4 bands are 0.5577, 0.3179, 0.0899, 0.0163, 0.3105, 0.0995, 0.3287, 0.1847 and 0.0509, which agree well with the semi-empirically calculated data of 0.58, 0.32, 0.09, 0.01, 0.31, 0.11, 0.34, 0.18 and 0.06, respectively [17]. In addition, the obtained Franck-Condon factors involving $\upsilon' = 0$–5 to $\upsilon'' = 0$–4 transitions compare favourably with those calculated by de Brouchere et al. [37], e.g., some relatively large Franck-Condon factors corresponding to the 0–0, 0–1, 1–0, 1–2 and 1–3 bands in this work are 0.5577, 0.3179, 0.3105 and 0.3287, respectively. Correspondingly, the theoretical results [37] of these bands are 0.5425, 0.3380, 0.3704, 0.3062, respectively.

The $A^1\Pi$ state can also decay to the $C^1\Sigma^-$ state. Table 2 presents the spectroscopic parameters of this state, which are in good agreement with previous theoretical ones [31]. Only Floch et al. [26] observed the $C^1\Sigma^-$ state in the study of the perturbations in the $A^1\Pi$ state. No spectroscopic information was obtained except for $T = 43{,}048$ cm^{-1} and $B = 0.6003$ cm^{-1} of an unassigned vibrational level for this state. As depicted in Fig. 1, the small energy difference between the $A^1\Pi$ and $C^1\Sigma^-$ states means that the emissions from the $A^1\Pi$ state to the $C^1\Sigma^-$ state are not very strong. Moreover, the TDMs of this system (Fig. 2) are not large enough. Hence, the obtained transition probabilities are not large enough, some of which are collected in Table 5.

Using the calculated Einstein coefficients of the $A^1\Pi$-$X^1\Sigma^+$ and $A^1\Pi$-$C^1\Sigma^-$ systems, we calculate the radiative lifetimes for the first 15 vibrational levels of the $A^1\Pi$ state (Table 11). Due to the much larger Einstein coefficients of the $A^1\Pi$-$X^1\Sigma^+$ system than those of the $A^1\Pi$-$C^1\Sigma^-$ system, the radiative lifetimes of the $A^1\Pi$ state are essentially determined by the $A^1\Pi$-$X^1\Sigma^+$ transition. These radiative lifetimes of the $A^1\Pi$ state are several hundred nanoseconds for all the calculated vibrational levels. Experimentally, Hanle signal detection [62] provided the radiative lifetime of 227 ± 70 ns for $\upsilon' = 0$ of $A^1\Pi$ state at zero pressure. The theoretical radiative lifetime calculated by de Brouckere et al. [37] for $\upsilon' = 0$ is 742.4 ns. Our calculated one is 695.4 ns, which is in good agreement with the theoretical one [37], but larger than the experimental value [62]. In fact, in practical measurements, the $A^1\Pi$ state is most likely to be perturbed by the adjacent electronic states, especially the very nearby $D^1\Delta$ state, which may decrease the radiative lifetime. de Brouckere et al. [37] also pointed out that radiative lifetime increases with the increasing vibrational quantum number. The opposite result is obtained here. Most probably it is because de Brouckere et al. [37] only consider the Einstein coefficients for $(\upsilon', \upsilon'') = (0$–$4, 0$–$4)$, whereas Einstein coefficients involving higher vibrational levels υ' and υ'' are taken into account in this work.

The $D^1\Delta$ state is dominated by the $5\sigma^2 6\sigma^2 2\pi^3 7\sigma^2 3\pi^1 8\sigma^0$ electron configuration. The calculated spectroscopic parameters of the $D^1\Delta$ state are listed in Table 2, which agree well with some theoretical results [31,37]. However, no definite spectroscopic parameters of the $D^1\Delta$ state are obtained experimentally except for little information of the observed perturbation in the $A^1\Pi$ state [20,26].

As shown in Fig. 2, The curve of the TDM for the $D^1\Delta$-$A^1\Pi$ system is similar to that of the $A^1\Pi$-$C^1\Sigma^-$ system along the internuclear distance, which is not too surprising as the $D^1\Delta$ and $C^1\Sigma^-$ states have similar molecular orbital compositions, differing only in the coupling of the angular moments. The R_e of the $D^1\Delta$ state is very close to that of the $A^1\Pi$ state and they both possess deep potential wells. Hence, many transitions for this system should exist. Small TDM values of this system also show that these transitions should not be strong. The number of the Einstein coefficients, which are of the order of 10^3 and 10^2, is 147 and 429, respectively. Some of relatively large Einstein coefficients are presented in Table 5. In addition, radiative lifetime is relatively large for low-lying vibrational level of the $D^1\Delta$ state. So the $A^1\Pi$-$C^1\Sigma^-$ system can be observed, but with great efforts.

The $2^1\Pi$ state is formed after promotions of two electrons from the $2\pi 7\sigma$ MOs into the 3π MO. This state can undergo dipole-allowed transitions to all of the lower singlet $A^1\Pi$, $X^1\Sigma^+$, $C^1\Sigma^-$ and $D^1\Delta$ states. As shown in Fig. 2, the curve of TDM for the $2^1\Pi$-$A^1\Pi$ system takes up a large area relative to the R_e-axis. So many intense emissions should exit for this system. Table 5 presents some relatively large Einstein coefficients and Franck-Condon factors for this system. Due to the large energy separation (Fig. 1) and large TDMs (Fig. 2) between $2^1\Pi$ and $X^1\Sigma^+$ states, there are a great deal of intense emissions for the $2^1\Pi$-$X^1\Sigma^+$ system. For the $2^1\Pi$-$C^1\Sigma^-$ and $2^1\Pi$-$D^1\Delta$ systems, the curves of TDM are similar, with relatively large values in the Franck-Condon region. Large Einstein coefficients are obtained near diagonal matrix elements for these two systems.

Overall, the $A^1\Pi$-$X^1\Sigma^+$, $2^1\Pi$-$A^1\Pi$, $2^1\Pi$-$X^1\Sigma^+$, $2^1\Pi$-$C^1\Sigma^-$ and $2^1\Pi$-$D^1\Delta$ systems should not be difficult to measure by appropriate experiments. The $A^1\Pi$-$C^1\Sigma^-$ and $D^1\Delta$-$A^1\Pi$ systems can also be detected with some efforts. Among the transitions from $2^1\Pi$ state to the lower $A^1\Pi$, $X^1\Sigma^+$, $C^1\Sigma^-$ and $D^1\Delta$ states, the emissions of the $2^1\Pi$-$X^1\Sigma^+$ system are most intense, followed by those of the $2^1\Pi$-$A^1\Pi$ system.

3.2. Radiative transitions between triplet states

Of the triplet states of PN, the $d^3\Delta$, $e^3\Sigma^-$ and $b^3\Pi$ states were identified by Saraswathy and Krishnamurty [21] from observation of the perturbations in the $\upsilon = 0$–4 levels of the $A^1\Pi$ state. Spectroscopic parameters of the $e^3\Sigma^-$ and $b^3\Pi$ states were also fitted by the observed energy levels lying at $\upsilon = 0$–4 levels of the $A^1\Pi$ state. So explicit vibrational levels of the $e^3\Sigma^-$ and $b^3\Pi$ states were not obtained. In order to compare our results with the experimental data, the calculated vibrational energy levels of the $e^3\Sigma^-$ and $b^3\Pi$ states approximately lying at υ=0–4 levels of the $A^1\Pi$ state are used to fit the spectroscopic parameters, which are given in Table 7, together with the experimental data [21]. Although the energy levels may be not consistent with the observed ones, relatively good agreement is observed for the $e^3\Sigma^-$ and $b^3\Pi$ states. The spectroscopic parameters of the $d^3\Delta$ state are not given because the large discrepancy between the calculated spectroscopic parameters and the experimental ones [21]. It is worth noting that our calculated spectroscopic parameters of the $d^3\Delta$ state agrees well with those calculated by Grein and Kapur [31] and those computed by Abbiche et al. [44]. Moreover, a larger active space does not improve the spectroscopic parameters of the $d^3\Delta$ state. So new experiments are needed to clarify such difference.

As shown in Fig. 3, the TDMs of the $b^3\Pi$-$a^3\Sigma^+$ and $b^3\Pi$-$d^3\Delta$ systems are relatively large over a wide range of internuclear distance. Moreover, the R_e of the $b^3\Pi$ state is close to that of the $a^3\Sigma^+$ state and that of the $d^3\Delta$ state. The energy separation between the $b^3\Pi$ and $a^3\Sigma^+$ states is large, whereas the T_e of the $b^3\Pi$ state is slightly larger than that of the $d^3\Delta$ state. Based on these results, Franck-Condon principle predicts that the emissions of the $b^3\Pi$-$a^3\Sigma^+$ system should be stronger than those of the $b^3\Pi$-$d^3\Delta$ system. Our calculated Einstein coefficients and Franck-Condon factors verify such prediction. Some large ones are listed in Table 8.

Due to the symmetry limitation, The $e^3\Sigma^-$ state can only spontaneously decay to the $b^3\Pi$ state. The $e^3\Sigma^-$-$b^3\Pi$ system has similar TDMs to those of the $b^3\Pi$-$a^3\Sigma^+$ and $b^3\Pi$-$d^3\Delta$ systems, which can be explained by the same electron configuration of the $e^3\Sigma^-$ state as those of the $a^3\Sigma^+$ and $d^3\Delta$ states.

The $2^3\Delta$ state can spontaneously decay to the $b^3\Pi$ and $d^3\Delta$ states. As seen in Fig. 3, the TDM of the $2^3\Delta$-$b^3\Pi$ system is near zero in the Franck-Condon region, which is not surprising as the two states differ by two electronic orbitals: the electron con-

figuration of the $2^3\Delta$ state is $5\sigma^2 6\sigma^2 2\pi^2 7\sigma^2 3\pi^2 8\sigma^0$, while the $b^3\Pi$ state is dominantly described by the $5\sigma^2 6\sigma^2 2\pi^4 7\sigma^1 3\pi^1 8\sigma^0$ electron configuration. There are only a few large Einstein coefficients which are of the order of 10^2. In general, this system should be hard to observe. The emissions of the $2^3\Delta-1^3\Delta$ system are strong. Some large Einstein coefficients and Franck-Condon factors are given in Table 9.

The $2^3\Sigma^-$ state is located at 62,436.04 cm^{-1}. The depth of the potential is 17,798.26 cm^{-1}, which carries 44 vibrational levels. This state can decay radiatively to the lower $1^3\Sigma^-$ and $b^3\Pi$ states. The vibrational band origins show that the emissions of the $2^3\Sigma^- - 1^3\Sigma^-$ system lie in the UV, visible and infrared regions. These emissions are relatively strong, but intense emissions between low-lying states mainly locate in the UV and visible regions. So it should not be difficult to observe the $2^3\Sigma^- - 1^3\Sigma^-$ system by a suitable experiment. Similar to the $2^3\Delta$-$b^3\Pi$ system, the $2^3\Sigma^-$-$b^3\Pi$ system corresponds to the $2\pi^2 7\sigma^2 3\pi^2$-$2\pi^4 7\sigma^1 3\pi^1$ transitions. Large Einstein coefficients occur in the bands corresponding to high υ' and low υ'' and they are in the UV band. Thus, The $2^3\Sigma^-$-$b^3\Pi$ system can be observed with great efforts.

In general, the $b^3\Pi$-$a^3\Sigma^+$, $e^3\Sigma^-$-$b^3\Pi$, $2^3\Delta-1^3\Delta$ and $2^3\Sigma^- - 1^3\Sigma^-$ systems should not be difficult to observe via appropriate spectroscopic techniques. The $2^3\Sigma^-$-$b^3\Pi$ and $b^3\Pi$-$d^3\Delta$ systems can also be measured with some efforts. Emissions of the $2^3\Delta$-$b^3\Pi$ system, however, should be difficult to obtain experimentally.

3.3. Radiative transitions between quintet states

The $1^5\Sigma^+$ state is predicted to lie at 44,095.84 cm^{-1} with a potential well of 7717.77 cm^{-1}, which supports 24 vibrational levels. The $1^5\Pi$ state is found at 53,760.81 cm^{-1}. It possesses a well depth of 9303.92 cm^{-1}. At the icMRCI+Q/56+CV+DK level of theory, the calculated spectroscopic parameters of the $1^5\Sigma^+$ and $1^5\Pi$ states are given in Table 2 and match well with recent theoretical ones [44].

As shown in Table 4, both the $1^5\Pi$ and $1^5\Sigma^+$ states have single reference configuration in nature around their corresponding equilibrium internuclear distances. The leading electronic transition between the two states is $2\pi^3 7\sigma^1$-$2\pi^2 7\sigma^2$ promotion. As displayed in Fig. 3, TDMs of the $1^5\Pi-1^5\Sigma^+$ system are relatively large in the Franck-Condon region. According to the Franck-Condon principle, the emissions of this system are expected to be relatively strong. Our calculations confirm this expectation with the fact that there are 59 and 119 emissions whose Einstein coefficients are of the order of 10^4 and 10^3, respectively. In addition, radiative lifetimes of all the vibrational levels for the $1^5\Pi$ state are relatively small (Table 11). Considering the factors above, we infer that the $1^5\Pi-1^5\Sigma^+$ system should not be difficult to detect by means of spectroscopy.

4. Conclusions

Utilizing the PECs calculated at the icMRCI+Q/56+CV+DK level of theory and the TDMs calculated by the icMRCI/AV6Z method, we have determined the vibrational band origins, Einstein coefficients and Franck-Condon factors for dipole-allowed transition systems between the $X^1\Sigma^+$, $A^1\Pi$, $C^1\Sigma^-$, $D^1\Delta$, $2^1\Pi$, $a^3\Sigma^+$, $b^3\Pi$, $d^3\Delta$, $e^3\Sigma^-$, $2^3\Delta$, $2^3\Sigma^-$, $1^5\Sigma^+$ and $1^5\Pi$ states, and have evaluated the vibrational radiative lifetimes of the $A^1\Pi$, $D^1\Delta$, $2^1\Pi$, $b^3\Pi$, $e^3\Sigma^-$, $2^3\Delta$, $2^3\Sigma^-$ and $1^5\Pi$ states. Several main conclusions have been reached below.

(1) The $2^1\Pi$-$A^1\Pi$ system covers a wide spectral range from UV to far-infrared region. The $2^1\Pi$-$X^1\Sigma^+$ system extends from vacuum UV to visible band. The $2^3\Delta$-$D^1\Delta$ system spreads from UV to mid-infrared wavelengths. The $1^5\Pi-1^5\Sigma^+$ system mainly lies in the VUV region. The spectral range are in the UV band for the $A^1\Pi$-$X^1\Sigma^+$, $2^1\Pi$-$C^1\Sigma^-$, $2^1\Pi$-$D^1\Delta$, $2^3\Delta$-$b^3\Pi$ and $2^3\Sigma^-$-$b^3\Pi$ systems, and in the infrared region for the $A^1\Pi$-$C^1\Sigma^-$, $D^1\Delta$-$A^1\Pi$, $b^3\Pi$-$a^3\Sigma^+$, $e^3\Sigma^-$-$b^3\Pi$ and $b^3\Pi$-$d^3\Delta$ systems. All these spectral ranges can be used to provide information for measuring these systems in the experiments.

(2) Spectral emissions of the $A^1\Pi$-$X^1\Sigma^+$, $2^1\Pi$-$A^1\Pi$, $2^1\Pi$-$X^1\Sigma^+$, $2^1\Pi$-$C^1\Sigma^-$, $2^1\Pi$-$D^1\Delta$, $b^3\Pi$-$a^3\Sigma^+$, $e^3\Sigma^-$-$b^3\Pi$, $2^3\Delta-1^3\Delta$, $2^3\Sigma^- - 1^3\Sigma^-$ and $1^5\Pi-1^5\Sigma^+$ systems should not be difficult to observe experimentally. Spectral emissions of the $A^1\Pi$-$C^1\Sigma^-$, $D^1\Delta$-$A^1\Pi$, $2^3\Sigma^-$-$b^3\Pi$ and $b^3\Pi$-$d^3\Delta$ systems can also be detected with some efforts. Whereas spectral emissions of the $2^3\Delta$-$b^3\Pi$ system should be difficult to measure according to Franck-Condon principle.

(3) Radiative lifetimes of the vibrational levels are about tens of nanoseconds for the $2^1\Pi$ state, about several hundred nanoseconds for the $A^1\Pi$ state and about several to tens of microseconds for the $b^3\Pi$, $2^3\Delta$, $2^3\Sigma^-$ and $1^5\Pi$ states. Such short radiative lifetimes mean that the spontaneous transitions from these states can easily occur. Radiative lifetimes of the vibrational levels for the $e^3\Sigma^-$ state about several to several hundred microseconds. Radiative lifetimes are very long for the lower vibrational levels of the $D^1\Delta$ state.

(4) Large transition parameters of several band systems are calculated and presented in this work, which can help in line identification and diagnostics of astrophysical plasma.

Acknowledgement

We acknowledge the support from the National Natural Science Foundation of China under Grant No. 51421063.

Supplementary material

Supplementary material associated with this article can be found, in the online version, at doi:10.1016/j.jqsrt.2019.02.002.

References

[1] Ziurys LM. Detection of interstellar PN: the first phosphorus-bearing species observed in molecular clouds. Astrophys J 1987;321:L81.
[2] Turner BE, Bally J. Detection of interstellar PN: the first identified phosphorus compound in the interstellar medium. Astrophys J 1987;321:L75–LL9.
[3] Irvine WM, Avery LW, Friberg P, Matthews HE, Ziurys LM. Newly detected molecules in dense interstellar clouds. Astrophys Lett Comm 1988;26:167.
[4] Turner BE, Tsuji T, Bally J, Guelin M, Cernicharo J. Phosphorus in the dense interstellar medium. Astrophys J 1990;365:569–85.
[5] Tenenbaum ED, Woolf NJ, Ziurys LM. Identification of phosphorus monoxide ($X^2\Pi_r$) in VY Canis Majoris: detection of the first PO bond in space. Astrophys J 2007;666:L29–32.
[6] Ziurys LM, Schmidt DR, Bernal JJ. New circumstellar sources of PO and PN: the increasing role of phosphorus chemistry in oxygen-rich stars. Astrophys J 2018;856:169.
[7] Beck ED, Kamiński T, Patel NA, Young KH, Gottlieb CA, Menten KM, Decin L. PO and PN in the wind of the oxygen-rich AGB star IK Tau. Astron Astrophys 2013;558:132–40.
[8] Fontani F, Rivilla VM, Caselli P, Vasyunin A, Palau A. Phosphorus-bearing molecules in massive dense cores. Astrophys J 2016;822:30.
[9] Rivilla VM, Fontani F, Beltrán MT, Vasyunin A, Caselli P, MartínPintado J, Cesaroni R. The first detections of the key prebiotic molecule PO in star-forming regions. Astrophys J 2016;826:161.
[10] Mininni C, Fontani F, Rivilla VM, Beltrán MT, Caselli P, Vasyunin A. On the origin of phosphorus nitride in star-forming regions. Mon Not Roy Astron Soc 2018;476:L39–44.
[11] Lefloch B, Vastel C, Viti S, Jimenezserra I, Codella C, Podio L, Ceccarelli C, Mendoza E, Lepine JRD, Bachiller R. Phosphorus-bearing molecules in solar-type star-forming regions: first PO detection. Mon Not Roy Astron Soc 2016;462:3937–44.
[12] Rivilla VM, Jiménezserra I, Zeng S, Martín S, Martínpintado J, Armijosabendaño J, Viti S, Aladro R, Riquelme D, Requenatorres M. Phosphorus-bearing molecules in the Galactic Center. Mon Not Roy Astron Soc 2018:475.

[13] Curry J, Herzberg L, Herzberg G. Spectroscopic evidence for the molecule PN. J Chem Phys 1933;1:749.
[14] Ghosh PN, Datta AC. Das Bandenspektrum des Phosphornitrids. Zeitschrift für Physik 1934;87:500–4.
[15] Curry J, Herzberg L, Herzberg G. Spektroskopischer Nachweis und Struktur des PN-Moleküls. Zeitschrift Für Physik 1933;86:348–66.
[16] Raymonda J, Klemperer W. Molecular beam electric resonance spectrum of $^{31}P^{14}N$. J Chem Phys 1971;55:232–3.
[17] Moeller MB, Silvers SJ. Fluorescence spectra of PN and BF☆. Chem Phys Lett 1973;19:78–81.
[18] Coquart B, Prudhomme JC. A new electronic transition of the PN molecule. J Phys B-At Mol Opt Phys 1980;13:2251–4.
[19] Coquart B, Prudhomme JC. The $^1\Sigma^+$-$X^1\Sigma^+$ transition of the PN molecule. J Mol Spectrosc 1981;87:75–84.
[20] Ghosh SN, Verma RD, Vanderlinde J. A high resolution study of $A^1\Pi$-$X^1\Sigma$ transition of the PN molecule. Can J Phys 1981;59:1640–52.
[21] Saraswathy P, Krishnamurty G. Rotational analysis of $A^1\Pi$- $X^1\Sigma^+$ bands of $P^{14}N$ and $P^{15}N$: perturbatio studies in the $A^1\Pi$ state. Pramana 1987;29:53–77.
[22] Verma RD, Ghosh SN, Iqbal Z. New spectrum of the PN radical in the vacuum ultraviolet region. J Phys B-At Mol Opt Phys 1987;20:3961–74.
[23] Bredohl H, Dubois I, Macau-Hercot D, Remy F, Breton J, Esteva JM. Rydberg states of PN. J Mol Spectrosc 1992;156:292–5.
[24] Ahmad IK, Hamilton PA. The Fourier transform infrared spectrum of PN. J Mol Spectrosc 1995;169:286–91.
[25] Bredohl H, Breton J, Dubois I, Elafif A, Esteva JM, Macauhercot D, Remy F, Saouli A, Some E. The absorption spectrum of PN between 1000 and 600 Å. J Mol Spectrosc 1995;171:125–9.
[26] Floch ACL, Melen F, Dubois I, Bredohl H. A new study of the perturbations in the $A^1\Pi$ State of PN. J Mol Spectrosc 1996;176:75–84.
[27] Cazzoli G, Cludi L, Puzzarini C. Microwave spectrum of $P^{14}N$ and $P^{15}N$: spectroscopic constants and molecular structure. J Mol Struct 2006;780:260–7.
[28] Gingerich KA. Gaseous phosphorus compounds. III. Mass spectrometric study of the reaction between diatomic nitrogen and phosphorus vapor and dissociation energy of phosphorus mononitride and diatomic phosphorus. Med I Dyn Fluid Monit 1969;73:2734–41.
[29] Hoeft TE, Törring T. Rotationsspektrum des PN. Zeitschrift Für Naturforschung A 1972;27:703–4.
[30] Gottscho RA, Field RW, Lefebvre-Brion H. Ab initio and semiempirical estimates of PN valence state interactions. J Mol Spectrosc 1978;70:420–31.
[31] Grein F, Kapur A. The electronic spectrum of PN. A configuration interaction study. J Mol Spectrosc 1983;99:25–34.
[32] Pyykkö P, Diercksen GHF, Müller-Plathe F, Laaksonen L. Fully numerical hartree-fock calculations on the third-row diatomics AlF, SiO, PN, CS, BCl, SH^- and P_2. Chem Phys Lett 1987;134:575–8.
[33] Peterson KA, Woods RC. Configuration interaction potential energy and dipole moment functions for thirteen 22 electron diatomics. J Chem Phys 1990;92:6061–8.
[34] Wong MW, Radom L. ChemInform abstract: isoelectronic analogues of PN: remarkably stable multiply charged cations. J Chem Phys 1990;21:638–44.
[35] de Brouckere G, Feller D, Koot JJA, Berthier G. Configuration interaction calculations on the $X^1\Sigma^+$ ground state and low-lying $A^1\Pi$ and $^1\Delta$ excited states of the PN molecule. I. Potential energy curve of the $X^1\Sigma^+$ state of PN. Miscellaneous spectroscopic observables. J Phys B-At Mol Opt Phys 1992;25:4433–45.
[36] Mclean AD, Liu B, Chandler GS. Computed self-consistent field and singles and doubles configuration interaction spectroscopic data and dissociation energies for the diatomics B_2, C_2, N_2, O_2, F_2, CN, CP, CS, PN, SiC, SiN, SiO, SiP, and their ions. J Chem Phys 1992;97:8459–64.
[37] de Brouckere G, Feller D, Koot JJA. Configuration interaction calculations on the $X^1\Sigma^+$ ground state and low-lying $A^1\Pi$ and $^1\Delta$ excited states of the PN molecule. II. Potential energy curves of the $A^1\Pi$ and $^1\Delta$ excited states of PN and spectroscopic properties. J Phys B-At Mol Opt Phys 1993;26:1915.
[38] Woon DE, Dunning TH. Benchmark calculations with correlated molecular wave functions. VI. Second row A2 and first row/second row AB diatomic molecules. J Chem Phys 1994;101:8877–93.
[39] Peterson KA, Dunning TH. Accurate correlation consistent basis sets for molecular core–valence correlation effects: the second row atoms Al–Ar, and the first row atoms B–Ne revisited. J Chem Phys 2002;117:10548–60.
[40] Kemeny AE, Francisco JS, Dixon DA, Feller D. Accurate ab initio study of the energetics of phosphorus nitride: heat of formation, ionization potential, and electron affinity. J Chem Phys 2003;118:8290–5.
[41] Coriani S, Marchesan D, Gauss J, Hättig C, Helgaker T, Jørgensen P. The accuracy of ab initio molecular geometries for systems containing second-row atoms. J Chem Phys 2005;123:913.
[42] Muniz EP, Jorge FE. HF and MP2 calculations on CN^-, N_2, AlF, SiO, PN, SC, ClB, and P_2 using correlated molecular wave functions. Int J Quantum Chem 2006;106:943–51.
[43] Yorke L, Yurchenko SN, Lodi L, Tennyson J. Exomol molecular line lists – VI. A high temperature line list for phosphorus nitride. Mon Not Roy Astron Soc 2014;445:1383–91.
[44] Abbiche K, Salah M, Marakchi K, Kabbaj OK, Komiha N. Ab initio study of PN electronic states – a qualitative interpretation of the perturbation and predissociation effects on observed transitions. Mol Phys 2014;112:117–26.
[45] NIST. https://physicsnistgov/PhysRefData/ASD/levels_formhtml.
[46] Knowles PJ, Werner HJ. An efficient second-order MCSCF method for long configuration expansions. Chem Phys Lett 1985;115:259–67.
[47] Knowles PJ, Werner HJ. An efficient method for the evaluation of coupling coefficients in configuration interaction calculations. Chem Phys Lett 1988;145:514–22.
[48] Werner HJ, Knowles PJ. An efficient internally contracted multiconfiguration reference CI method. J Chem Phys 1988;89:5803–14.
[49] Werner H-J, Knowles PJ, Knizia G, Manby FR, Schütz M. WIREs Comput Mol Sci 2012;2:242–53. doi:10.1002/wcms.82.
[50] Werner H-J, Knowles PJ, Knizia G, Manby FR. MOLPRO, a package of ab initio programs http://www.molpronet.
[51] Woon DE, Dunning TH. Gaussian basis sets for use in correlated molecular calculations. IV. Calculation of static electrical response properties. J Chem Phys 1993;98:1358–71.
[52] Mourik TV, Wilson A, Dunningjr T. Benchmark calculations with correlated molecular wavefunctions. XIII. Potential energy curves for He2, Ne2 and Ar2 using correlation consistent basis sets through augmented sextuple zeta. Mol Phys 1999;96:529–47.
[53] Truhlar DG. Basis-set extrapolation. Chem Phys Lett 1998;294:45–8.
[54] Reiher M, Wolf A. Exact decoupling of the Dirac Hamiltonian II. The generalized Douglas-Kroll-Hess transformation up to arbitrary order. J Chem Phys 2004;121:10945–56.
[55] Reiher M, Wolf A. Exact decoupling of the Dirac Hamiltonian. I. General theory. J Chem Phys 2004;124:64102.
[56] de Jong WA, Harrison RJ, Dixon DA. Parallel Douglas-Kroll energy and gradients in NWChem: estimating scalar relativistic effects using Douglas-Kroll contracted basis sets. J Chem Phys 2001;114:48–53.
[57] Laux CO, Kruger CH. Arrays of radiative transition probabilities for the N_2 first and second positive, NO β and γ, N_2^+ first negative, and O_2 Schumann-Runge band systems. J Quant Spectrosc Radiat Transf 1992;48:9–24.
[58] da Silva ML, Dudeck M. Arrays of radiative transition probabilities for CO_2–N_2 plasmas. J Quant Spectrosc Radiat Transf 2006;102:348–86.
[59] Roy RJL. LEVEL: a computer program for solving the radial Schrödinger equation for bound and quasibound levels. J Quant Spectrosc Radiat Transf 2017;186:167–78.
[60] Wyse FC, Manson EL, Gordy W. Millimeter wave rotational spectrum and molecular constants of $^{31}P^{14}N$. J Chem Phys 1972;57:1106–8.
[61] Wang J, Sun J, Shi D. Accurate ab initio study of low-lying electronic states of phosphorus nitride radical. Chin Phys B 2010;19:340–6.
[62] Moeller MB, Mckeever MR, Silvers SJ. Hanle effect measurement of the lifetime of the $A^1\Pi$ state of PN. Chem Phys Lett 1975;31:398–400.